

Clemson University TigerPrints

All Theses

Theses

8-2010

Surface characterization and electrochemical behavior of colloidal particles

Cinta Pepin

Clemson University, cintapepin@hotmail.com

Follow this and additional works at: https://tigerprints.clemson.edu/all_theses

 Part of the [Materials Science and Engineering Commons](#)

Recommended Citation

Pepin, Cinta, "Surface characterization and electrochemical behavior of colloidal particles" (2010). *All Theses*. 889.
https://tigerprints.clemson.edu/all_theses/889

This Thesis is brought to you for free and open access by the Theses at TigerPrints. It has been accepted for inclusion in All Theses by an authorized administrator of TigerPrints. For more information, please contact kokeefe@clemson.edu.

SURFACE CHARACTERIZATION AND ELECTROCHEMICAL BEHAVIOUR OF COLLOIDAL PARTICLES

A Thesis
Presented to
the Graduate School of
Clemson University

In Partial Fulfillment
of the Requirements for the Degree
Master of Art/Science
Materials Science and Engineering

by
Cinta Pepin
August 2010

Accepted by:
Prof. Stephen H. Foulger, Committee Chair
Prof. Kathleen C. Richardson
Prof. Vincent Blouin
Prof. Evelyne Fargin
Prof. Véronique Jubéra
Prof. Jean-Louis Bobet
Prof. Mona Treguer-Delapierre

ABSTRACT

There is an ongoing interest in research focused on developing polymeric organic-light-emitting-devices (OLED) to replace inorganic devices. Compared to inorganic devices, OLEDs could present better properties such as higher efficiency, lower cost and simpler device fabrication. In an attempt to get a device with high efficiency, the hole transporting group and the electron transporting group were combined into a polymer to make an individual “particle device”. The idea was to create a polymer particle containing both charge transporting moieties via emulsion polymerization. In this presentation, different techniques will be described that were used to determine the stability and the surface characterization of the colloidal particles (zeta potential, conductometric titration for the surface charge density). Equally as important for OLED devices is the control of the energy profile of the material, or the transferred energy within the device. Cyclic voltammetry was used to measure the electrochemical behavior of the charge transporting particles. To this end, cyclic voltammetry is very useful to determine the HOMO-LUMO energy levels and the band gap energy.

ACKNOWLEDGMENTS

I would like to thank Prof. Stephen Foulger who welcomed me in his group and allowed me to do this internship; all my research group and more particularly Micheal Daniele, Ali Foguth, Ryan Roeder and Parul Rungta for all their help.

I also would like to thank Prof. Kathleen Richardson and Prof. Evelyne Fargin for this opportunity that they gave me to enter in this dual master; my committee members, Prof. Vincent Blouin, Prof. Kathleen Richardson, Prof. Jean-Louis Bobet, Prof. Evelyne Fargin, Prof. Véronique Jubéra and Prof Stephen Foulger.

My acknowledgements are going to Mrs. Kathy Bolton, Mrs. Adeline Barre, Miss Leslie Bilger and Mrs Shelby Sherrif for all their precious help for the administrative part of this new master.

TABLE OF CONTENTS

	Page
TITLE PAGE	i
ABSTRACT.....	ii
ACKNOWLEDGMENTS	iii
LIST OF TABLES	v
LIST OF FIGURES	vi-vii
 CHAPTER	
I. Introduction and motivation.....	1
1. Introduction.....	1
2. Motivation.....	6
II. Experimental procedures, results and discussion.....	8
1. Zeta Potential	8
1.1 Experimental procedure and results.....	10
2. Charge density	13
2.1 Experimental procedure and results.....	14
3. Cyclic voltammetry	18
3.1 Experimental procedure	21
3.2 Results for poly(vinylcarbazole).....	22
3.3 Results for PA particles with carbazole moieties	24
3.4 Results for poly(acrylate) containing an oxadiazole moiety.	27
3.5 Results for PA particles with oxadiazole moieties	29
III. Conclusion	33
REFERENCES	35

LIST OF TABLES

Table		Page
1.1	Table 1. Summary of the HOMO, LUMO and band gap energy levels for the PVK and PA particles with clicked carbazole	27
2.1	Table 2. Summary of the HOMO, LUMO and band gap energy levels for the poly(2-(biphenyl-4-yl)-5-(4-tert-butylphenyl)-1,3,4-oxadiazole and PA particles with clicked oxadiazole.	30

LIST OF FIGURES

Figure	Page
1.1 Figure 1 Schematic of typical thin film organic light emitting device (OLED) configuration	4
1.1 Figure 2 Schematic of the oxadiazole moiety	4
2.1 Figure 3 Schematic of the carbazole moiety	4
2.1 Figure 4 Schematic of the emulsion polymerization and the “click” reaction	5
2.1 Figure 5 Schematic of the double layer and the surface of the shear plane where the zeta potential is measured	10
2.1 Figure 6 Zeta potential of a solution of poly(styrene) particles.....	11
2.1 Figure 7 Zeta potential of a solution of poly(propargyl acrylate) particles .	12
2.1 Figure 8 Titration of 38 mL of HCl solution at 0.01M.....	15
2.1 Figure 9 Titration of PS particles in DI water with NaOH solution	17
2.1 Figure 10 Titration of PA particles in DI water with NaOH solution	17
2.1 Figure 11 Cyclic voltammogram of poly(vinyl carbazole) film.....	23
2.1 Figure 12 Absorption spectra of PVK recoded between 200and 600 nm....	23

2.1	Figure 13 Comparison of cyclic for a) PA particles and b) PA particles with the clicked carbazole	25
2.1	Figure 14 Comparison of absorption spectra or a) carbazole molecules and b) PA particles with the clicked carbazole	26
2.1	Figure 15: Cyclic voltammogram of the poly(2-(biphenyl-4-yl)-5-(4-tert-butylphenyl)-1,3,4-oxadiazole) film	28
2.1	Figure 16: Absorption spectra of the poly(2-(biphenyl-4-yl)-5-(4-tert-butylphenyl)-1,3,4-oxadiazole).....	29
2.1	Figure 17 Comparison of cyclic voltammograms for a) PA particles and b) PA particles with the clicked oxadiazole	31
2.1	Figure 18 Comparison of absorption spectra for a) oxadiazole molecules and b) PA particles with the clicked oxadiazole.....	32

CHAPTER ONE

Introduction and motivation

I-1. Introduction

In the early 1990s, Burroughes² developed the first polymer-based light emitting diodes (LED) device employing a π -conjugated polymer. Conjugated polymers are organic semiconductors, due to the π molecular orbitals which are delocalized along the polymer chain, and are often referred to as intrinsically conductive polymers (ICP). These ICPs can respond to an electronic excitation whereby the injection of an electron and a hole into the conjugated chain leads to an excited state which can then decay radiatively. The potential for high photoluminescence efficiency in organic molecular semi-conductors has generated an interest in the light emission of organic semi-conductors in devices through charge injection under a high applied field, specifically electroluminescent devices. The main advantage over non-polymeric organic semi-conductors is the possibility of processing the polymer to form useful and robust structures. Through the control of the design of the polymer, there are excellent possibilities for the development of this class of materials in a range of electroluminescence applications.² The other advantages of working with organic materials are the ease of device fabrication, low material cost, low environmental impact, facile synthesis routes and high rates of improvement in luminous efficiency. A typical Organic Light Emitting Device (OLED)

consists of a hole-injecting electrode, a hole-transport layer, an emissive layer, an electron-transport layer and an electron-injecting electrode. Electrons and hole are injected into the device from the electrodes, recombine in the light-emitting layer, creating an excited state that decays to the ground state by emitting a photon. To construct an OLED with optimal efficiency and device lifetime, holes and electrons must be injected into the device at a rate to achieve similar densities of the two carriers. To have good performance, the devices fabricated using organic small molecules or insoluble ICP in a multilayer configuration require long and complex protocols and fabrication techniques like costly high-vacuum deposition techniques. An alternative to the use of a multilayer device is to use a single layer in which an electroluminescent (EL) species is embedded in a hole and electron transporting-host (cf. **Figure 1**). This methodology may take the form of mixing an EL dye with individual hole- and electron-transporting materials. In this approach, research has been conducted with a hole transporting material (poly(9-vinylcarbazole), (PVK)), blended with an electron transporting molecule (2-(4-tert-Butylphenyl)-5-(4-biphenyl)-1,3,4-oxadiazole) (PBD), and a fluorescent or phosphorescent dye. In this case, there is a risk of phase separation and crystallization due to the non-uniform distribution of the electron transport molecule and that can degrade the device performance. To solve this problem, the solution found was to copolymerize the hole- and electron-transporting groups into a copolymer and then prevent phase separation and crystallization. The hole- and electron- transporting groups were carbazole and oxadiazole moieties. A methyl methacrylate derived copolymer functionalized with pendant carbazole and oxadiazole moieties as a single

layer device was presented with different ratios to explore the photoluminescence and electroluminescence of the system.^{3,4} With the same idea of an electroluminescent dye embedded in a hole and electron transporting polymer host, researchers elaborate electroluminescent colloidal particles that can produce a wide range of emission colors. This approach exploits the concept that the particles in a colloidal based OLED can be viewed as individual “particle-devices”. Those particle devices are composed of a carbazole-oxadiazole luminescent dye system that will emit a single-color. By sequestering the emissive species, one can create single layer devices that emit light on the wavelengths across the visible spectrum and create the desired emission by mixing the different “single-color dispersions” in particular Red/Green/Blue ratios.^{5,6} The research group I am working with is now developing the synthesis of aqueous-phase nanoparticles. These are surface-functionalized with emissive moieties through a “click chemistry” approach^{1,7,8}. Click transformations (i.e. click chemistry), specifically the copper(I)-catalyzed reaction between azides and terminal alkynes to form the stable heterocyclic linker, 1,4-disubstituted 1,2,3- triazole⁹, have found acceptance in the materials science community. Azides and alkynes are relatively inert to various solvents (including water), molecular oxygen, and common reaction conditions in organic synthesis, and these advantages are particularly useful for attaching multi-functional molecules to surfaces^{1,9-11}. The stability of azides and alkynes in aqueous solutions enables these functionalities to act as inert chemical handles for a range of selective chemical reactions, and in particular, offers a simple route to modify particles composed of semiconductor^{1,12,13}, metallic, or biological/organic materials. This study demonstrated

the attachment of the azide-functionalized small molecules, oxadiazolyl and carbazolyl moieties (**Fig 2&3**), on poly(propargyl acrylate) (PA) particles. Oxadiazolyl and carbazolyl moieties are utilized for their electron and hole transporting properties respectively. The PA particles present, at their surface, alkyls groups which are reactive groups. Alkynes group at the surface of the PA are the reactive sites for the “click” reaction with the azides at the end of the carbazole and oxadiazole molecules (**Fig 4**).⁷

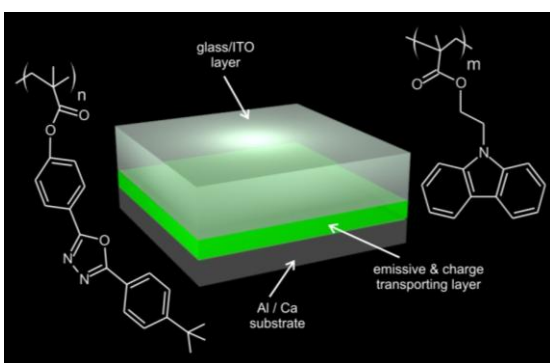


Figure 1 Schematic of a typical thin film organic light emitting device (OLED). Device utilizes poly(methyl methacrylate)-derived homo- & co-polymers with pendant carbazole and oxadiazole moieties for charge transportation.

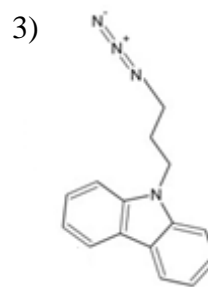
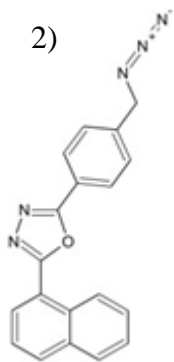


Figure 2 & 3: Schematic of the oxadiazole (2) and the carbazole (3) moieties that are “clicked” on the alkynes groups at the surface of the PA particles through their azides end groups.

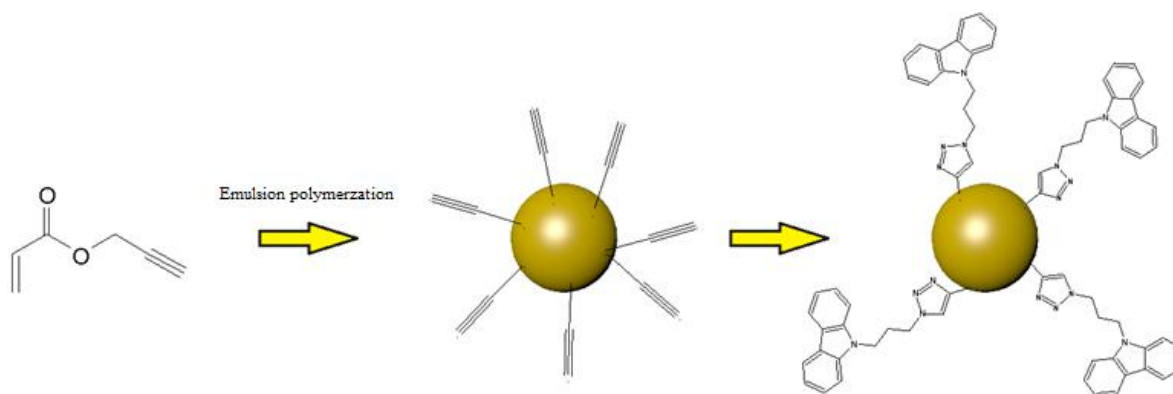


Figure 4: Schematic of the emulsion polymerization of the propargyl acrylate monomer into a polymer particle and the “click” reaction of an carbazole molecule on the surface of the poly(propargyl acrylate) particles¹.

In that case, the main application targeted is in the medical domain, for the diagnostic value of early detection of some diseases with contrast agents. The main interest for that kind of particles is the development of fluorobes to achieve selective imaging sensitivity by using nanoparticles doped with an emitting species.¹

Previous work using this same system (polymer with carbazole and oxadiazole) were studied but it was films of polymers and not particles. It is the fact that the structure is changing that we want to study and maybe see the some effects on the electrochemical properties.

I-2. Motivation

In order to understand the behavior of poly(propargyl acrylate) (PA) particles with surface-attached hole- and electron-transporting moieties and transition them into optical applications, it is essential to characterize their colloidal stability and optical properties. Since these particles are in colloidal suspensions, their intrinsic stability in solution and particle charge density are essential parameters that must be characterized. Suspensions of charged colloidal particles in aqueous media are frequently used and enhancing their stability against aggregation is very important. Emulsion synthesized particles in solution are charged due to residual initiator fragments as well as copolymerized ionic monomers and this charge gives the particles their stability in solution. That is why I was interested in determining the zeta potential and charge density of the poly(propargyl acrylate) (PA) particles used in this current work. The effective electrical charge on particles can be determined using different electrokinetic techniques, such as, electrophoretic mobility, streaming current or potential and electric conductivity¹⁴. Zeta-potential plays an important role in the electrokinetic characterization of solid–liquid interfaces; it is a very important parameter for colloids or nanoparticles in suspension. The zeta potential of a particle cannot be measured directly but is deduced

from experimental techniques (electrophoretic mobility) with the help of theoretical approaches¹⁵. It determines the electric potential of a particle at a precise area from the particle surface, often termed the surface of the shear plane. The potential measured at this plane is referred to as the zeta potential. Its value is closely related to the suspension's stability and particle surface morphology. Another property related with the characterization of the surface of the particles is the charge density, or charge per unit area on the surface of the particle. These charges are the result of the synthesis of the particles and are unique in magnitude for each colloidal suspension. Conductometric titration is the technique by which we can determine the number of charges on each particle and the corresponding final charge density of the particles.

The second phase of my research has focused on the optical and electrochemical properties of the oxadiazole and carbazole surface modified PA particles. It is well known that the energy profile in the various layers of an organic light emitting device (OLED) is a critical design parameter in the successful operation of the device⁴. Parameters such as ionization potential (IP), electronic affinity (AE) and energy gap (E_{gap}) are important to understand and control the electrical and optical properties of conducting polymers. These parameters are useful to construct the energy level diagrams of conducting polymers¹⁶. The redox reactions in the conducting polymers are responsible for the electrical conductivity as well as for the electrochemical and electrochromic properties of these materials. Those properties are easily obtained through cyclic voltammetry studies. With the help of different techniques of characterization (cyclic voltammetry and UV-VIS spectroscopy), the electrochemical properties of the

different electroluminescent moieties (carbazole and oxadiazole) on the PA particles were investigated.

CHAPTER TWO

Experimental procedures, results and discussions

II-1.Zeta potential

Zeta potential is the abbreviation for electrokinetic potential in colloidal system. Its value can be related to the stability of the colloidal dispersion¹⁷. There are always charges at the surface of the particles, and when those particles are dispersed in a liquid, the net charge at the particles surface will affect the ion distribution in the nearby region and increases the concentration of the counter ions close to the surface. An electrical double layer is formed in the region of the particle-liquid interface. The particles and the double layer are called the electrokinetic unit. The zeta potential is defined as the electrical potential at the surface of the shear plane. The surface of the shear is defined as the separation between the electrokinetic unit and the bulk solution. A high zeta potential will confer stability: the dispersion will resist aggregation. When the zeta potential is low, attraction exceeds repulsion and the dispersion will break and flocculate. A general rule is

that a colloidal system is stable due to the mutual electrostatic repulsion of the particles when the absolute value of the zeta potential is greater than 30mV⁷.

The zeta potential is not measurable directly; it is calculated from the electrophoretic mobility^{14,15,18,19}. When the particles in solution are under an electric field, the charged particles will move toward the electrode of the opposite charge. The particles will move with a velocity proportional to the magnitude of the charge. The particles in solution will scatter the light from a laser beam and the frequency of the light scattered will be shifted because of the movement of the particles. The frequency shift is measured as the particles mobility and this mobility is then converted to the zeta potential through Henry's equation¹⁷:

Eq 1:
$$\zeta = \frac{3}{2} \frac{\eta \mu_e}{\varepsilon \varepsilon_0 f(ka)}$$

Where ζ is the zeta potential, μ_e the electrophoretic mobility, ε the dielectric constant, ε_0 the dielectric permittivity of vacuum, k the Debye-Hückel screening parameter and

$$f(ka) = 1 + \frac{1}{2} \left(1 + \frac{2.5(1 + 2 \exp(-ka))}{ka} \right)^{-3}.$$

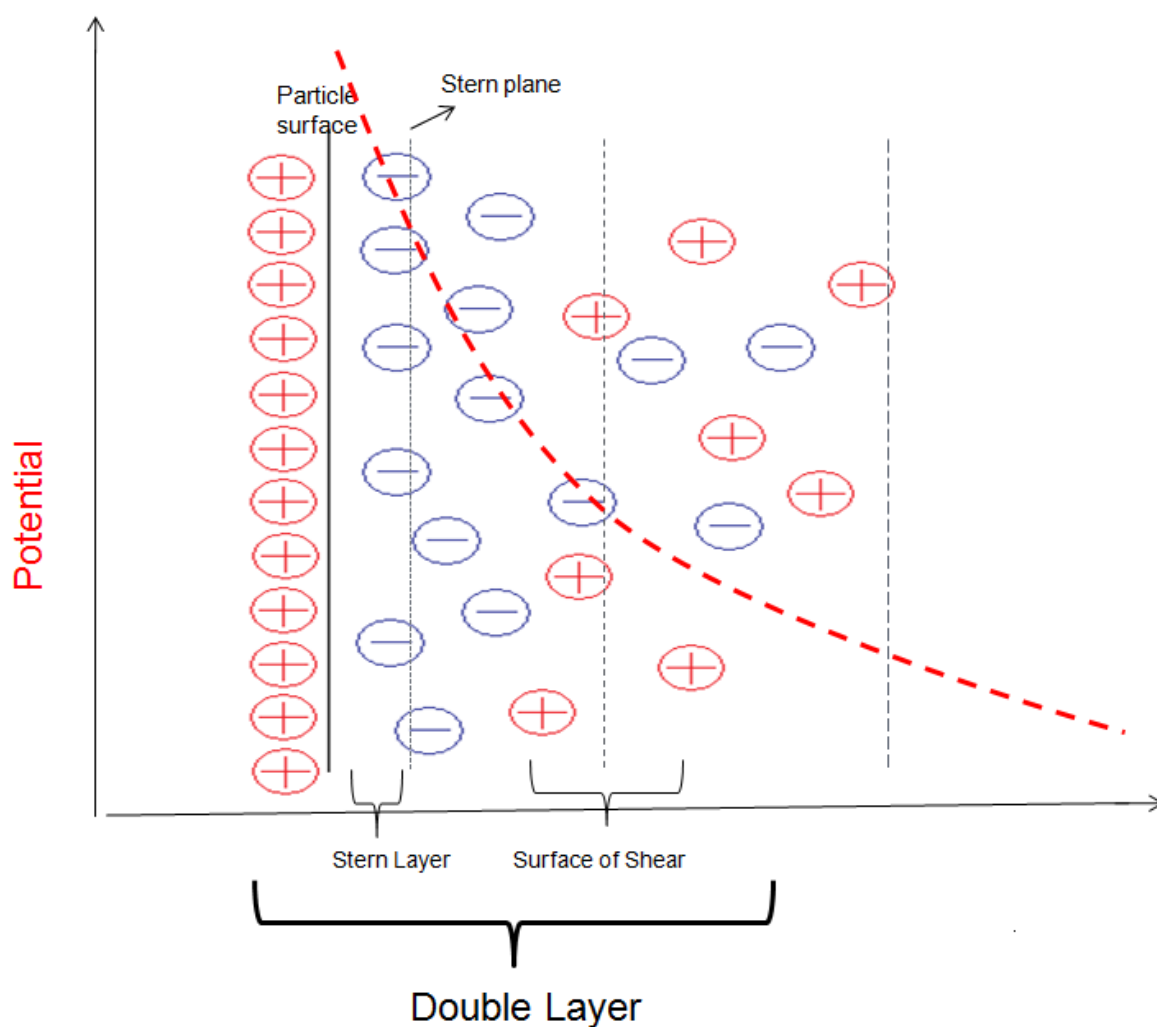


Figure 5: Schematic of the distribution of the counter ions near to the surface of the particle, with the determination of the double layer and the surface of the shear plane where the zeta potential is measured.

II.1.1. Experimental procedure and results:

Before doing the zeta potential on the poly(propargyl acrylate) (PA) particles, the experiment was carried out on poly(styrene) (PS) particles in order to get used to the

technique and reproduce results that have been demonstrated in different papers²⁰⁻²². The zeta potential of the particles was measured over a range of pH values with a ZetaPlus zeta potential analyzer (Brookhaven Instruments Corp.).

The zeta potential of a solution of poly(styrene) particles was studied in KCl solution (0.001M) through a range of pH which was changed by adding NaOH (0.1M) and HCl (0.1M) solutions^{23,24} to the colloidal mixture. **Figure 6** shows the zeta potential of PS particles for different pH between 9 and 2. We can see the decrease of the zeta potential as long as the solution becomes more acidic. The absolute values of the zeta potential stay under 30 mV until pH 3 but after that, at around a pH of 2 the particles are no longer stable.

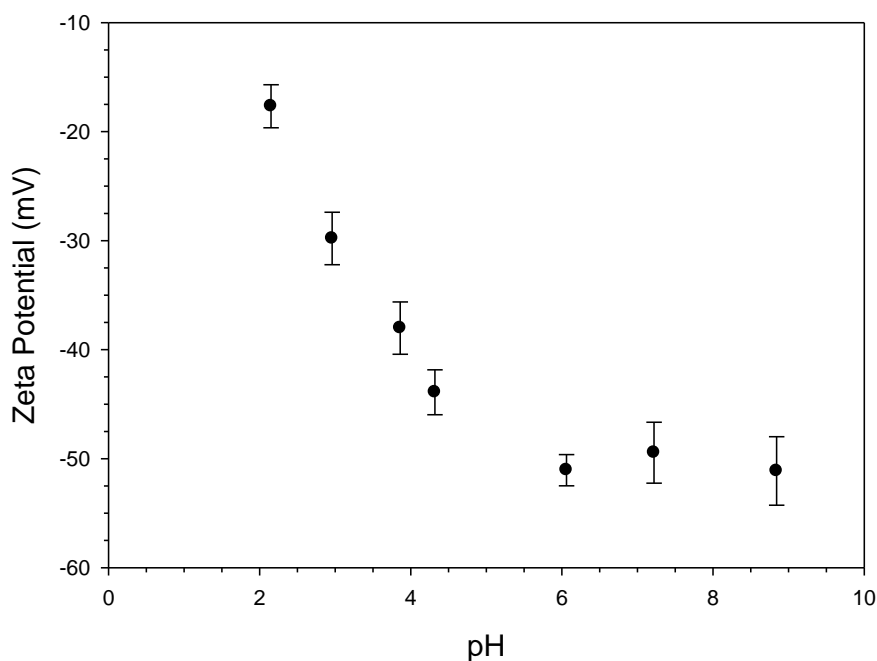


Figure 6 : Zeta potential of a solution of poly(styrene) particles in KCl solution (0.001M) through a range of pH.

The same experiment has been done on poly(propargyl acrylate) ⁷ particles and the results have been reported on **Figure 7**. We notice that even though the zeta potential of the PA particles decreases with the pH, it stays at lower values than -30 mV which means that the particle solution is still stable at low pH.

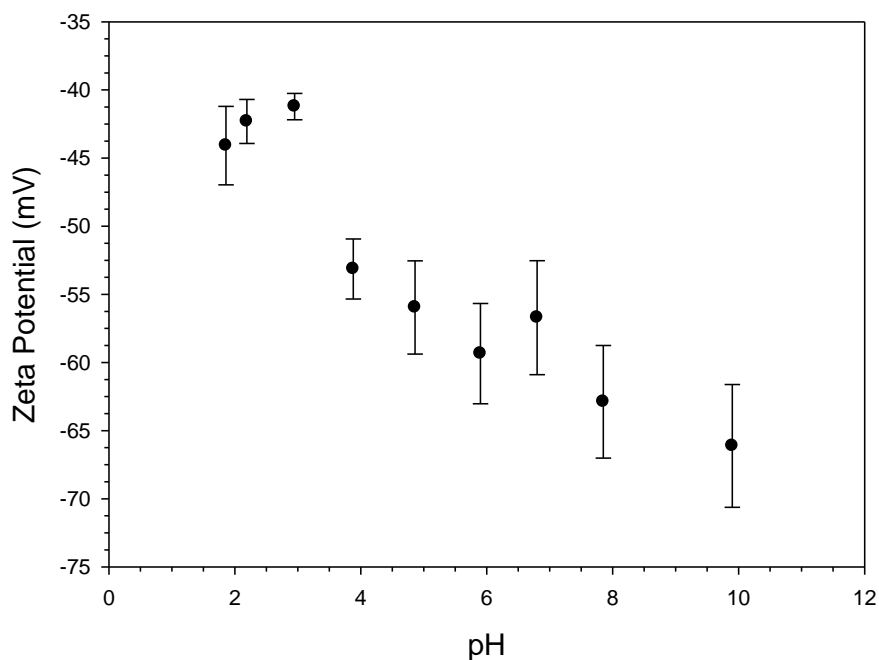


Figure 7 : Zeta potential of a solution of poly(propargyl acrylate) particles in KCl solution (0.001M) through a range of pH.

The errors bars seen on the Zeta potential results correspond to the standard deviation given directly by the equipment due to the multiple runs into a cycle of experiment. The size of the particles was verified at different pH by DLS in order to be sure that the system is still monodisperse

II-2. Surface charge density

We define the “surface charge” or “surface charge density” as the total charge at the surface of the particles measured by titration. An ideal model colloid should comprise monodisperse spherical particles stabilized with a known number of chemically bound surface groups. To use these latexes as model colloids, we must know the surface charge density of the particles. Conductometric titration is a basic technique for surface-charge determination^{25,26}. In the literature, there are numerous accounts of surface charge density analysis of poly(styrene) particles made by emulsion polymerization.^{25,27,28} At the end of the reaction and after a cleaning process²⁹, the surfaces of the particles are stabilized thanks to the sulfate end-groups of the polymer molecules. The goal of knowing the charge density is to determine the number of those sulfates end-groups. An easy way to calculate the number of those charges is to ion-exchange the solution with ion-exchange resin and then to carry out a conductometric titration on the particles with a basic solution. The ion-exchange resin will replace the sulfate end-groups with its H⁺ form and then we can directly titrate the H⁺ charges with the basic solution (NaOH solution). While we are adding NaOH solution in the particle solution, the conductivity decreases (OH⁻ reacting with the H⁺), once all the H⁺ have reacted the conductivity increases, and we find the equivalent point^{25,26}.

With the equivalent point, we can then calculate the charge density through:

Eq 2: Intrinsic charge =
$$\frac{\text{volume of a particle} * Na * V_{NaOH} * M_{NaOH}}{\text{Total volume solution} * \text{volume of particles solution}}$$

The charge density is calculated with a program in which we need to enter the diameter of the particles, the molarity of NaOH solution, the volume fraction of latex, the total volume of the mixture dispersion and the titration data points.

Even though each batch of polymers particles is different from another when we talked about charge density, the experiment was performed on poly(styrene) particles before being done on the PA particles. The conductivity of the polymer solutions were measured with a Brinkmann Metroohm. The equipment delivers automatically a preset amount of NaOH solution inside the particle solution and we let it stabilize before measuring the conductivity.

II.2.1. Experimental procedure and results:

First, calibration of the NaOH solution that will serve to titrate the different polymer dispersions was made. We prepare an aqueous solution of chloride acid of known concentration (0.01M) and titrate it with the basic solution while following the conductivity. At the equivalent point we can determine the concentration of the NaOH solution. On **Figure 8**, we can see both legs of the specific conductance-mL NaOH curve are linear, and the extrapolation to intersection gives the equivalence point. For this titration, the equivalent point at 27.10 mL allowed us to determine the concentration of the NaOH solution at 0.0132 M.

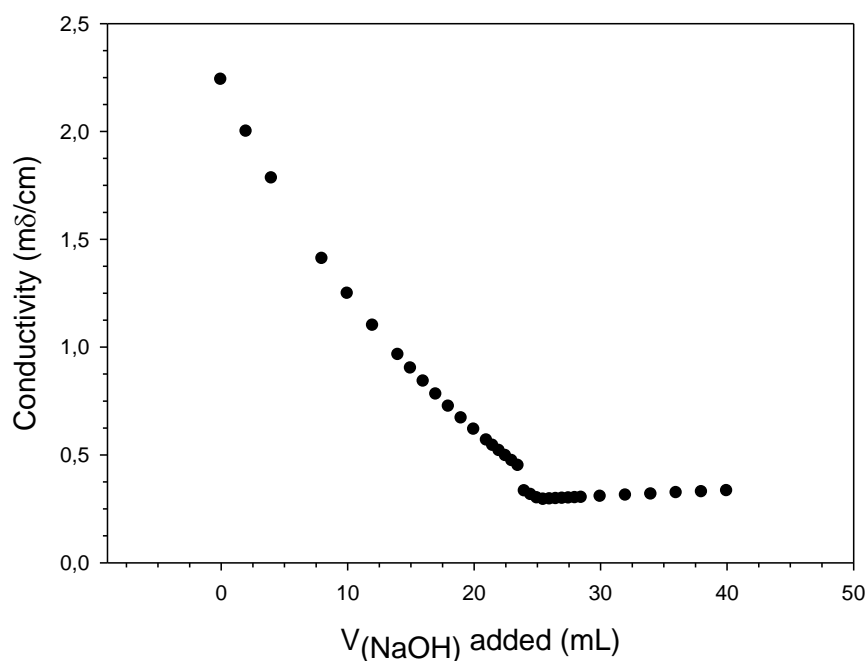


Figure 8: Titration of 38 mL of HCl solution at 0.01M .The equivalent point determined at 27.10 mL of NaOH added. Concentration of the basic solution calculated at 0.0132M.

The PS and PA particles were prepared using a standard aqueous emulsion polymerization technique with sodium dodecyl sulfate as the surfactant and potassium persulfate as the initiator¹. At the end of the reaction, the surfaces of the particles are negatively charged because of the adsorbed emulsifier and the sulfate end-groups of the polymer molecules. To remove the adsorbed emulsifier, the colloidal solution was cleaned against deionized water at 60°C using dialysis²⁹. At this point only the sulfate end-groups (SO_4^-) remain at the surface of the particles. The particles solution was then ion-exchanged with an ion-exchange resin to obtain the H^+ form on the surface of the particles. Thus their number can be determined by titration with a NaOH solution with a concentration of 0.0132M. Conductometric titration was performed on 2 mL samples of

cleaned particles (in 58 mL of deionized water), the titrations were done in a stirred vessel with continuous bubbling of N₂ using a conductivity dip cell and a conductivity meter. Similar to the titration of the NaOH solution, we observe in **Figures 9 and 10** the typical curve for conductometric titration. Both cases show a linear decreasing conductivity during the adding of OH⁻ in the solution and an increasing of the conductivity passing the equivalent point. For the PS particles (**Fig 9**), the equivalent point was determined at 15.8 mL and then the surface density was calculated through the program at 0.0232 μC/cm². The PA particles solution presents an equivalent point after 31.4 mL of NaOH added and a surface density of 0.025 μC/cm².

The rounded minimum is mainly due to slow attainment of equilibrium near the equivalence point. This shape of curve is typical of what we found in the titration of the strong-acid surface groups with a strong base. The differences between the titration of the charges on particles and the free charges are due to the immobility of the functional groups on the surface of the particles and to the reduced mobility of the counter-ions on the double layer^{25,30}.

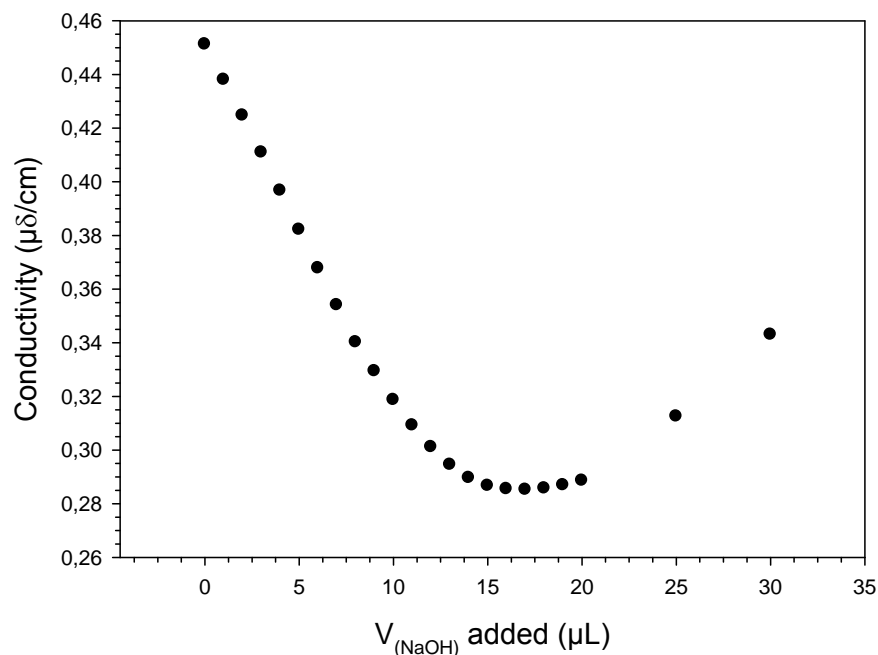


Figure 9: Titration of 2 mL of PS particles in 58 mL of DI water with NaOH solution under N_2 bubbling. Equivalence point at 15.8 mL of NaOH solution added for 2 mL of polymer solution. The surface charge was calculated at $0.0232 \mu C/cm^2$

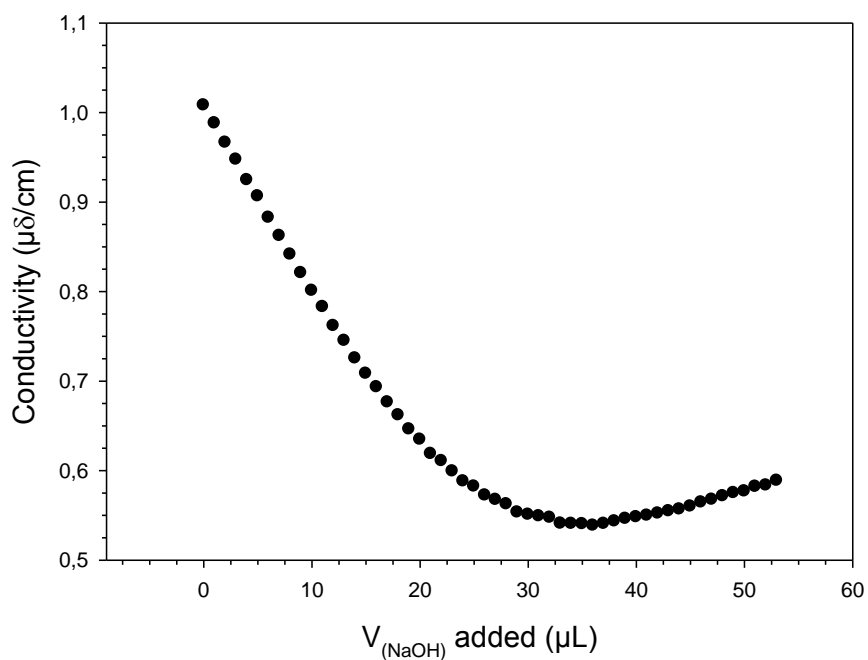


Figure 10: Titration of 2 mL of PA particles in 58 mL of DI water with NaOH solution under N_2 bubbling. Equivalence point at 31.4mL of NaOH solution added for 2 mL of polymer solution. The surface charge was calculated at $0.0225 \mu C/cm^2$

II-3. Cyclic Voltammetry

Cyclic voltammetry (CV) is an important technique that can be used to determine the energy profile of an organic material, and as applied in the current case, a polymer with charge transporting and fluorescent oxadiazole or carbazole moieties. In its simplest form, the technique manifests itself as cycling a potential across a sample and measuring the resulting current. The technique allows for the measurement and determination of the material's ionization potential (IP), electron affinity (AE) and electronic energy band gap (E_{gap}). The energy band gap is defined as the energy difference between the valence band and the conduction band. The ionization potential is the energy from the valence band edge to the vacuum level, and the electron affinity is the energy from the conduction band edge to the vacuum level. Although, conjugated polymers do not present a band as in inorganic crystalline semiconductors. They only have energy intervals with a high density of states that correspond to the HOMO (Highest Occupied Molecular Orbital) and the LUMO (Lowest Unoccupied Molecular Orbital)¹⁶. These properties can be related to simple reactions such as oxidation and reduction. The oxidation process corresponds to the removal of an electron from the HOMO (or IP) and the reduction process corresponds to the addition of an electron to the LUMO (or AE). With cyclic voltammetry, when the organic material shows a reversible reduction and oxidation reactions it is possible to determine all the energetic characteristics of the material, but in our case, the different polymers employed in our studies exhibit irreversibility when scanned. In this case, only the oxidation of the polymer will be used to determine the HOMO energy level. The

energy band gap will be determined optically by spectroscopy UV-VIS spectroscopy and the LUMO will be calculated from the two latter results through:

Eq 3:
$$\text{LUMO} = E_{\text{gap}} + \text{HOMO}.$$

During the cyclic voltammetry experiment, in the case of the oxidation process, no charge will be removed until the voltage applied reaches an onset value that corresponds to the highest occupied state in the valence band. The ionization potential was determined from this onset value of the oxidation. The onset point of oxidation E'_{ox} is determined graphically on the cyclic voltammogram by drawing two tangents at the rising oxidation current and the background current. To transpose the measured oxidation value (E'_{ox}) to the ionization potential, it is necessary to relate the electrochemical potential to the vacuum level relative to which the IP is defined. The potential value of the oxidation (E_{ox}) is referred to the standard hydrogen electrode (SHE) first and then corrected to the vacuum level reference. The conversion to the vacuum level of the SHE is about -4.6 eV^{16,31-33}.

Eq 4:
$$E_{\text{SHE}} = E_{\text{vac}} + 4.6$$

where E_{SHE} is the standard hydrogen electrode potential and E_{vac} the vacuum potential.

Then, we have to do the correction for the case that Ag/AgCl electrode is used as the reference electrode. The potential is expressed as:

Eq 5:
$$E_{\text{Ag/AgCl}} = E_{\text{SHE}} - 0.2 = E_{\text{vac}} + 4.4$$

Finally the oxidation potential (E_{ox}) onset relative to the vacuum level can be calculated:

Eq 6:
$$E_{\text{ox}} = E'_{\text{ox}} + E_{\text{Ag/AgCl}} = E'_{\text{ox}} + E_{\text{vac}} + 4.4$$

Assuming that $E_{\text{vac}} = 0 \text{ V}$,

Eq 7:
$$E_{ox} = E'_{ox} + 4.4$$

Then we can calculate the HOMO energy or IP:

Eq 8:
$$IP = -e \cdot E_{ox} = \text{HOMO}$$

where e is the elementary charge.

For all the polymers studied through CV analysis, the onset oxidation value (E'_{ox}) was determined graphically and the real value of the oxidation potential and IP value were calculated utilizing **Eqns.6-8**. Because of the non reversibility of this reaction^{16,34}, we cannot obtain the LUMO energy level in the same manner for determining the HOMO energy level. The alternative approach is to measure optically the energy band gap of the material by spectroscopy. The band gap energy of the different materials is determined by UV-VIS spectroscopy. The absorption spectra were recorded between 200 and 600 nanometers. The onset of the absorption¹⁶ corresponds to the energy of the band gap and can be determined graphically. With the determination of the band gap, we can calculate the LUMO energy through the use of **Eqn. 3**.

Those experiments were carried on different samples which involved the presence of carbazole or oxadiazole moieties which are well known to be used as hole and electron transport moieties respectively³⁴⁻³⁶. For the initial study, a polymer containing a carbazole moiety, poly(vinyl carbazole) (PVK), on a thin film was investigated. This first step was done in order to reestablish the technique on a thin film configuration which is the simplest way (to cyclic voltammetry in solution). The second phase of the study focuses on the signature of the carbazole moiety attached on the surface of poly(propargyl acrylate) (PA) particles. Those two steps allowed comparison of the signature of the

carbazole in different configurations, the first time as a polymer and the second time as a “clicked” moiety on the surface of a particle. Secondly, similar experiments were made with a polymer containing an oxadiazole moiety, the poly(2-(biphenyl-4-yl)-5-(4-tert-butylphenyl)-1,3,4-oxadiazole) on thin film and the oxadiazole at the surface of PA particles.

II.3.1. Experimental procedure:

A CH Instruments Model 660B electrochemical workstation was employed for acquiring cyclic voltammograms and for applying the requisite potential programs. The optical absorption data were acquired on a Perkin Elmer Lambda 900 UV/VIS/NIR spectrophotometer.

The different polymers with carbazole and oxadiazole moieties were drop-cast on an Indium-Tin-Oxide (ITO) coated glass slide to make a thin film for the cyclic voltammetry analysis. The same drop-casting systems were done for the solution of PA particles with the different moieties on it. The ITO coated glass is first cleaned with acetone and isopropyl alcohol and then plasma cleaned for 5 minutes. Once the ITO coated glass is cleaned, solutions of different samples were drop-casted and dried in ambient air.

The electrolyte used in this system is a solution of Tetrabutyl-amonium tetrafluoroborate (TBATFB) in acetonitrile with a concentration of 0.1M.

A set of three electrodes were used to record the cyclic voltammogram: a Platinum wire as a counter electrode, an Ag/AgCl wire as a reference electrode and the ITO coated glass

with the sample drop-casted on it as the working electrode. The electrode set-up is established in glass vial containing the electrolyte solution, and connected to the electrochemical work station. The solution is purged for 30 minutes with nitrogen gas to remove the oxygen and then the cyclic voltammogram was collected.

II.3.2. Results for Poly(vinyl carbazole):

The electrochemical characteristics of the poly(vinyl carbazole) (PVK) was the initial polymer studied and its CV characteristics are presented in **Figure 11**. For this study, the potential was cycled between -1.5 and 1.5 eV. From the CV curve, it is possible to determine graphically the onset potential of the oxidation E'_{ox} , which is in this case 0.9 V. By applying **Eqns. 6-8**, we can calculate the ionization potential and determine the HOMO level, which is -5.3eV for this homopolymer.

From the absorption spectrum of the polymer (cf. **Figure 12**), the onset of absorption for PVK occurs at 3.4 eV (364 nm), resulting in a LUMO energy level of -1.9 eV.

Those results can be put in correlation with others results reported in the literature³⁶⁻³⁸. In their paper^{34,36}, H. Macit reported the onset value of oxidation of carbazole (E'_{ox}) at 0.9V and H. Meng an onset oxidation value around 0.83V. The onset absorption for the PVK was also found around 360 nm in the paper of K. M. Yeh³⁸.

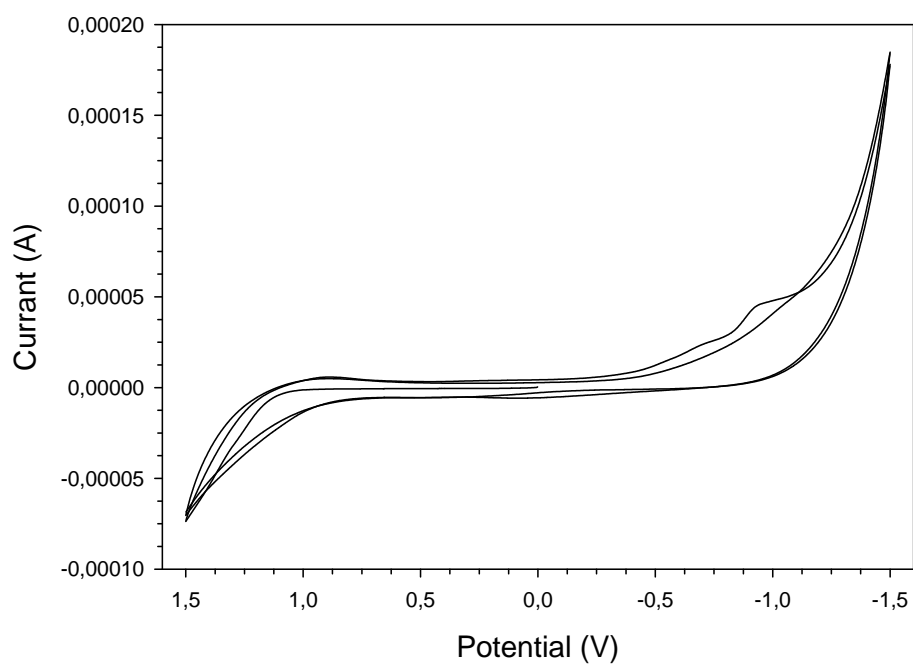


Figure 11: Cyclic voltammogram of poly(vinyl carbazole) film on ITO glass between -1.5 and 1.5 V with a scan rate of 0.01V/s. E'_{ox} determined at 0.9V, HOMO energy level calculated to be -5.3eV.

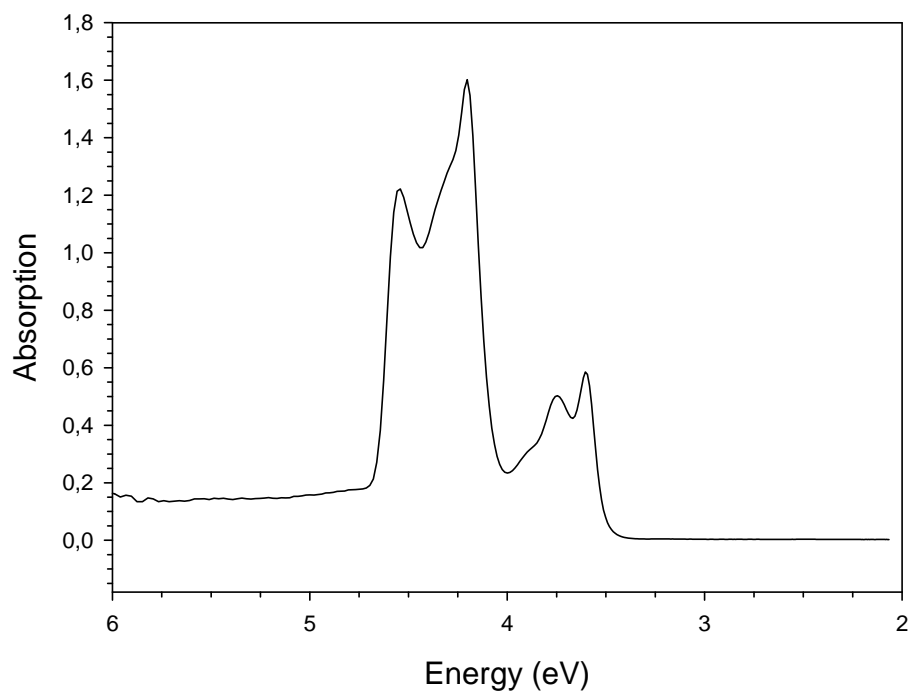


Figure 12: Absorption spectra of PVK recorded between 200 and 600 nm. Onset absorption value at 3.4 eV which equal to the energy of the band gap.

II.3.3 Results for PA Particles with carbazole moieties:

For those experiments, the study of PA particles without any moieties on it was done first to make sure that nothing happens in the area of the signature of the oxidation of the carbazole (i.e. around 1eV). Then cyclic voltammogram of PA particles with carbazole on it were recorded between -0.5V and 2V. Compare to cyclic voltammogram of the PA particles by themselves (**Fig 13-a**), we can observe the presence of a sharp peak at an onset value of 1.15V on **Figure 13-b**). The peak corresponds to the oxidation of the carbazole at the surface of the PA particles. The value of the HOMO energy level was calculated at -5.55eV which is close to the value we found for the carbazole as a polymer which was -5.3eV (**Fig 11**). For the UV-VIS spectroscopy of the particles, it is more difficult to identify the electronic band gap because of the scattering effect of the particles with the incoming laser beam. In order to be able to see the signature of the carbazole, we performed the experiment on the molecules of carbazole, the same that is “clicked” on the particles. Though, the results reported on **Figure 14** demonstrated that with a very dilute solution of clicked particles, we can get spectra with the same activation energy than the carbazole molecules alone. For the molecules of carbazole, the onset value of absorption is located at 3.4 eV (**Fig 14-a**)) which seems to correspond very well to the onset value of the particles of PA with carbazole (**Fig 14-b**)).

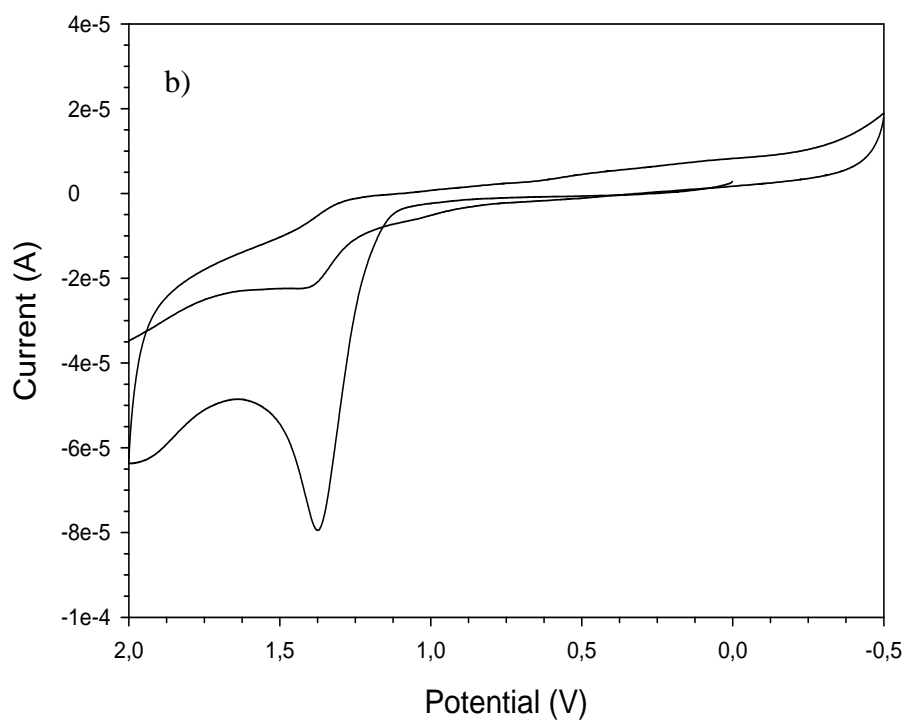
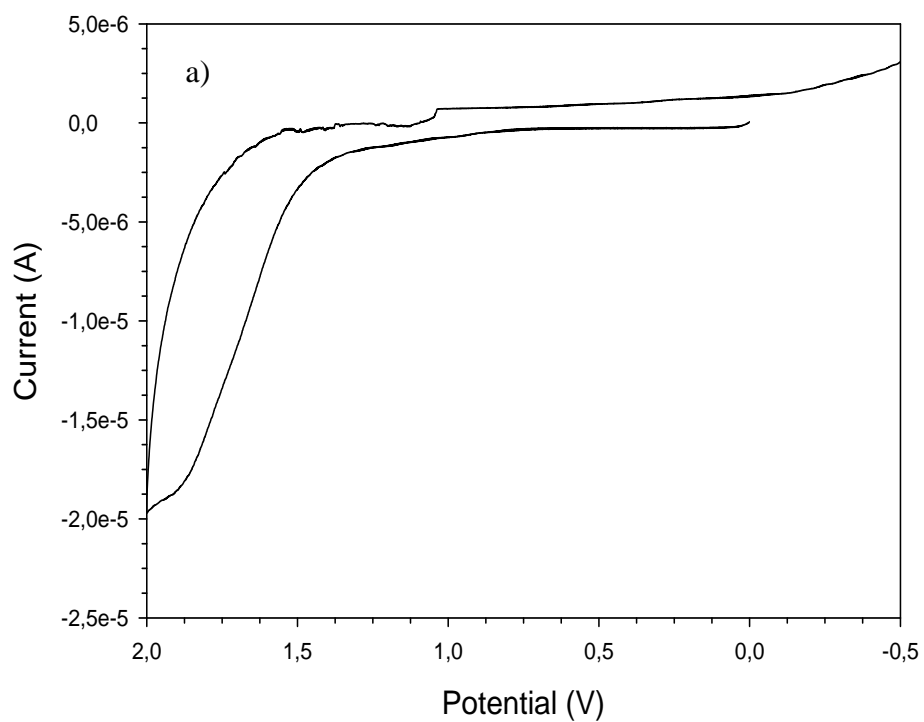


Figure 13: Comparison of cyclic voltammograms recorded between -0.5 and 2 V for a) PA particles and b) PA particles with the clicked carbazole. Fig 13-b) shows a broad peak for the oxidation of the carbazole at 1.15V which correspond to a HOMO energy level of -5.55 eV

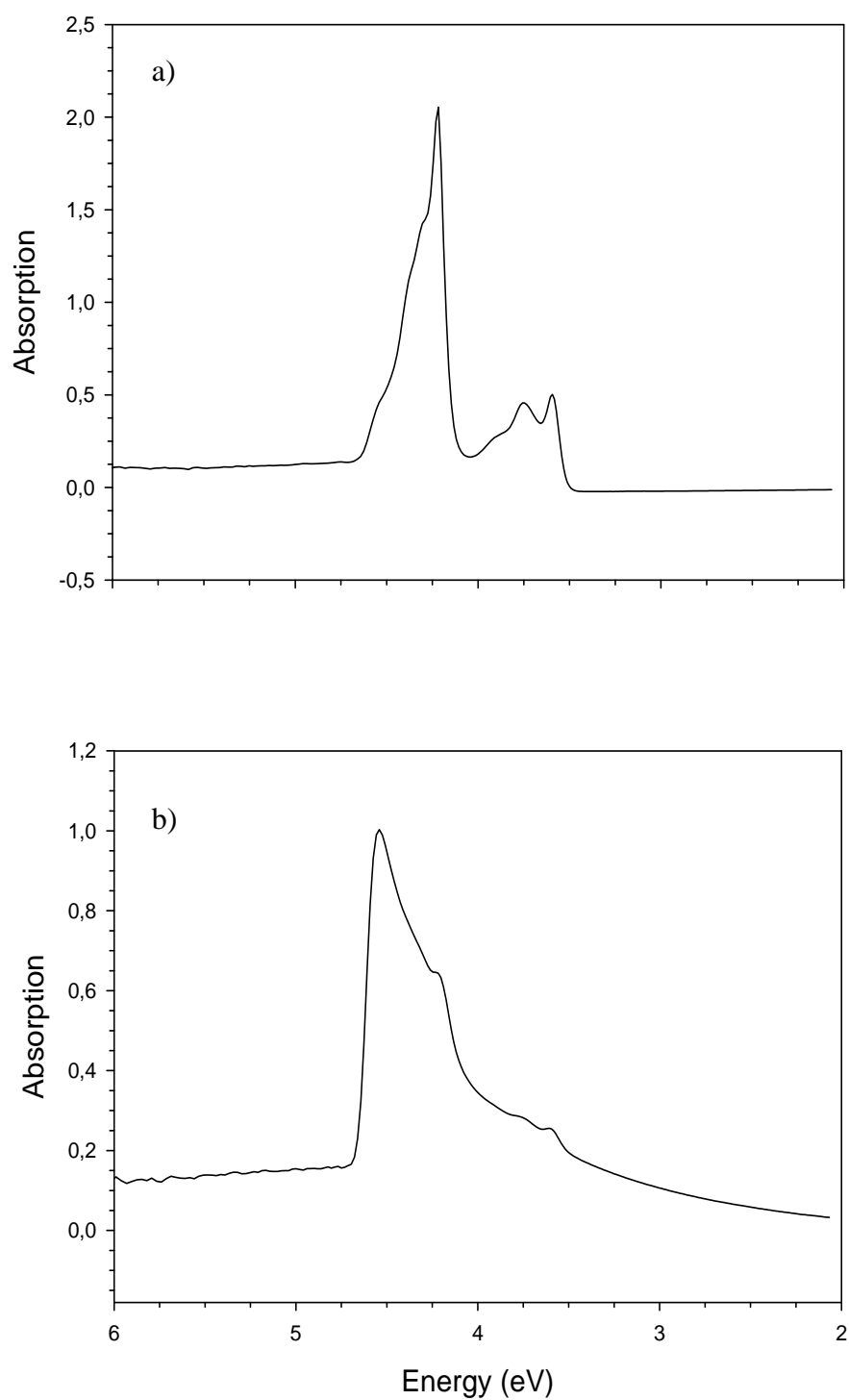


Figure 14: Comparison of absorption spectra recorded between 200 and 600 nm for a) carbazole molecules and b) PA particles with the clicked carbazole. Both spectra show an onset value of absorption at 3.5 eV which correspond to the energy band gap of the carbazole.

The different results obtained for the poly(vinyl carbazole) and the PA particles with clicked carbazole are summarized in **Table 1** with the values of the calculated LUMO for each case.

	E'_{ox} (V)	E_{ox} (V)	HOMO (eV)	E_{gap} (eV)	LUMO (eV)
Poly(vinylcarbazole)	0.90	5.30	-5.30	3.40	-1.90
PA particles with carbazole moieties	1.15	5.55	-5.55	3.5	-2.05

Table 1: Summary of the HOMO, LUMO and band gap energy levels for the PVK and PA particles with clicked carbazole.

II.3.4. Results for Poly(acrylate) containing an oxadiazole moiety:

For polymer, poly(2-(biphenyl-4-yl)-5-(4-tert-butylphenyl)-1,3,4-oxadiazole), the same process of electrochemical experiments were conducted as were done on the poly(vinyl carbazole). The cyclic voltammogram of a thin film of polymer on an ITO-coated-glass was recorded between -3V and 3V. As can be seen on **Figure 15**, the peak of the oxidation process for the oxadiazole, E'_{ox} , occurs at an onset value of 1.89 V. Combining this result with the absorption spectra deduced band gap (cf. **Figure 16**) for

this oxadiazole containing polymer, we can deduce HOMO energy level of 6.29 eV, while the electronic energy band gap is 3.44 eV. The resulting LUMO energy level is - 2.85 eV.

In the literature, a lot of references can be found about different polymers containing oxadiazole moiety³⁸⁻⁴⁵. Here, the results found for the HOMO energy level are lower than the ones referenced in the literature which are contained between -5.4 and -5.8 eV. The energy band gap however is comparable to the others results found in those papers which are contained between 3.3 and 3.7 eV.

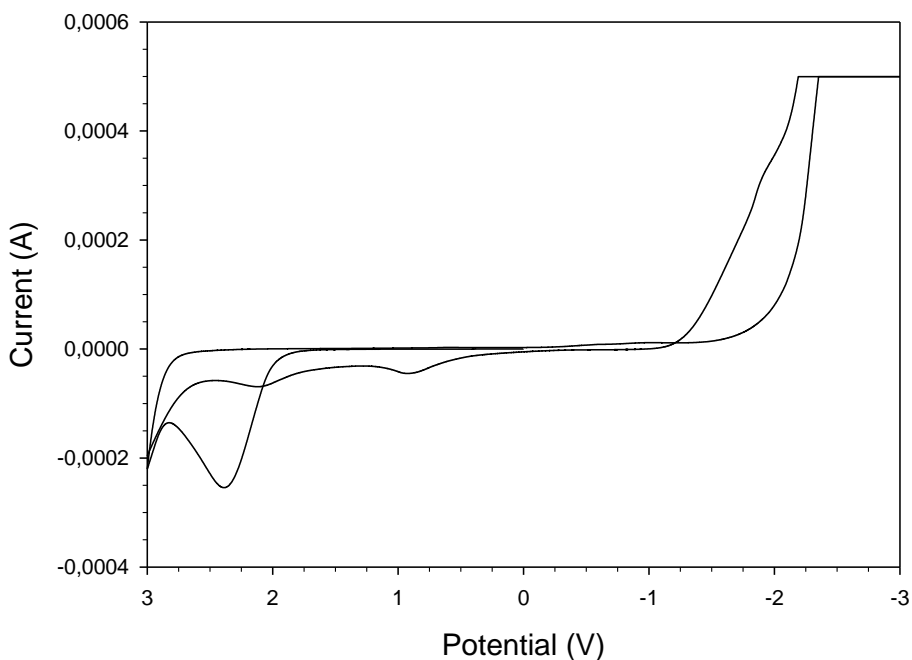


Figure 15: Cyclic voltammogram of poly(2-(biphenyl-4-yl)-5-(4-tert-butylphenyl)-1,3,4-oxadiazole) film on a ITO glass between -3 and 3 V with a scan rate of 0.01 V/s. E'_{ox} determined at 1.89V, HOMO energy level calculated to be at -6.29eV.

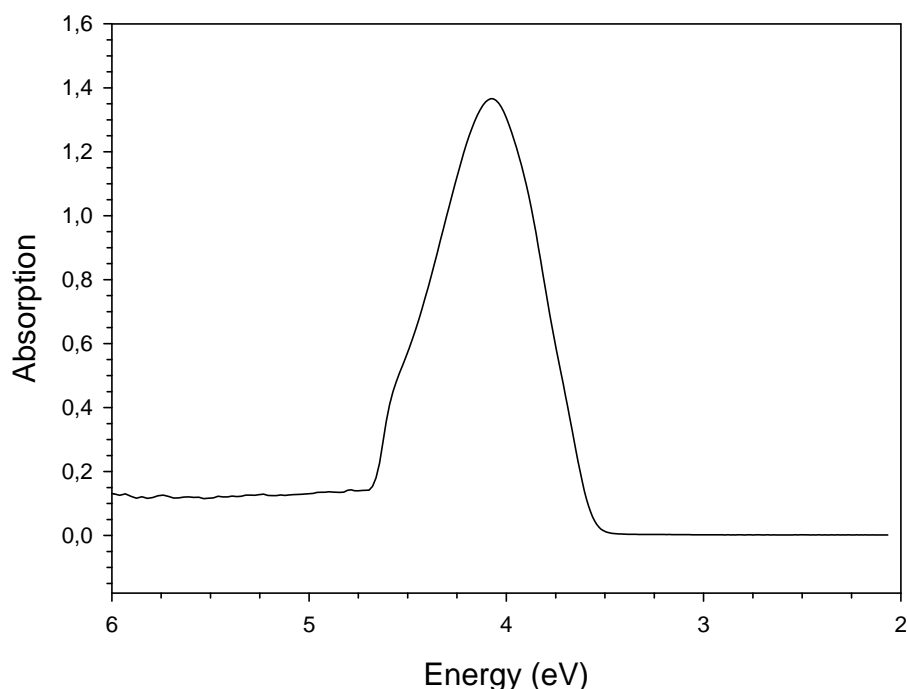


Figure 16: Absorption spectra of the poly(2-(biphenyl-4-yl)-5-(4-tert-butylphenyl)-1,3,4-oxadiazole) recorded between 200 and 600 nm. Onset absorption value at 3.44 eV which is equal to the energy of the band gap.

II.3.5. Results for PA Particles with oxadiazole moieties:

The cyclic voltammogram of PA particles with oxadiazole attached on the surface were recorded between -0.5V and 2V and compared to the cyclic voltammogram of the neat PA particles recorded under the same conditions. The **Figure 17** presents the results and the peak corresponding to the oxidation of the oxadiazole at the surface of the PA particles appears at 1.34 eV, resulting in a HOMO energy level of -5.74 eV. This result is not exactly the same as was found for the oxadiazole moiety containing polymer but it is

similar to the results found in the literature. F. Cacialli³⁹ and K. M. Yeh³⁸ report values of the HOMO energy level of oxadiazole at -5.72 and -5.77 eV. About the UV-VIS spectroscopy of the particles, the same procedure was adopted as was presented in the previous section. One complication in the use of the particles is the strong scattering that is encountered with small particles and therefore the absorption spectra of the particles is combined with the absorption spectra of the oxadiazole small molecule to find the electronic band gap. We first recorded the molecules of oxadiazole by it selves (**Fig 18-a**)) and in a second time clicked on the PA particles (**Fig 18-b**)). For both cases the onset value of the absorption spectra are similar and the energy band gap is deduced to be at 3.33 eV. The LUMO energy level was then calculated at -2.44 eV from **Equation 3**.

Table 2 presents the results collected for this study of the oxadiazole signature.

	E' _{ox} (V)	E _{ox} (V)	HOMO (eV)	E _{gap} (eV)	LUMO (eV)
Poly(oxadiazole)	1.89	6.29	-6.29	3.44	-2.85
PA particles with oxadiazole moieties	1.34	5.74	-5.74	3.33	-2.44

Table 2: Summary of the HOMO, LUMO and band gap energy levels for the poly(2-(biphenyl-4-yl)-5-(4-tert-butylphenyl)-1,3,4-oxadiazole and PA particles with clicked oxadiazole.

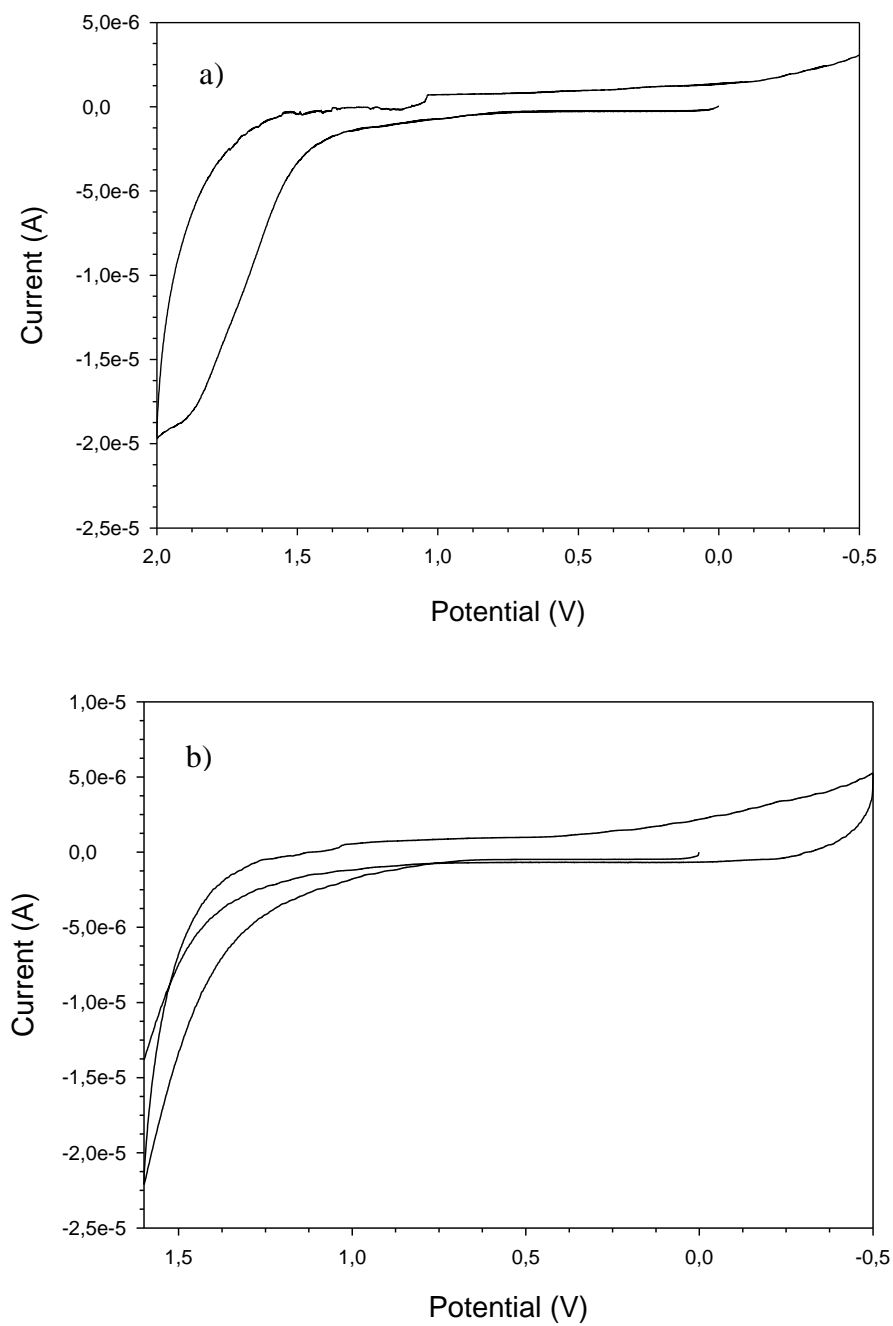


Figure 17: Comparison of cyclic voltammograms recorded between -0.5 and 2 V for a) PA particles and b) PA particles with the clicked oxadiazole. Fig 17-b) shows a peak for the oxidation of the carbazole at 1.34V which correspond to a HOMO energy level of - 5.74 eV

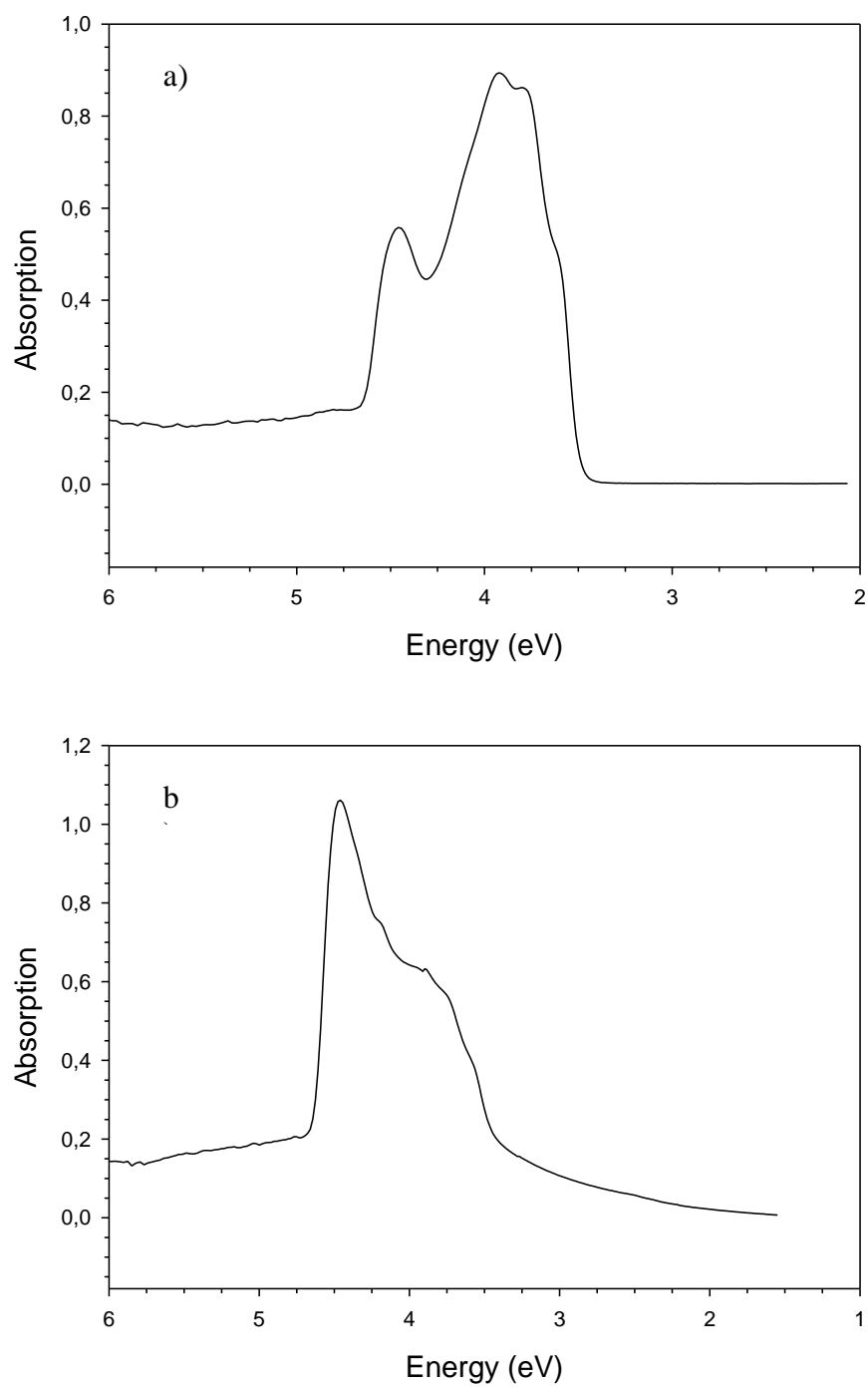


Figure 18: Comparison of absorption spectra recorded between 200 and 600 nm for a) oxadiazole molecules and b) PA particles with the clicked oxadiazole. Both spectra show an onset value of absorption at around 3.33 eV which correspond to the energy band gap of the oxadiazole.

CHAPTER THREE

Conclusion

During this project, the focus of the work was to determine and characterize two main properties for colloidal electroluminescent particles, specifically poly(propargyl acrylate) (PA) particles surface modified with oxadiazole and carbazole. In the first phase of the research, the stability and surface characterization of these particles were investigated by the determination of the zeta potential of the particles (potential of the particles in dilute solution at the surface of the shear plane) and the intrinsic charge density through a conductometric titration study. The Zeta potential results on the PA particles show absolute values under 30 mV which translate their stability over a range of pH and the conductometric titration allows us to determine a charge density to be ca. $0.025\mu\text{C}/\text{cm}^2$. Then, the electrochemical characterization of those particles was defined to understand their optical properties. The application of these particles in any final “particle-device” will consist of PA particles with hole- and electron-transporting moieties on the surface of the particles. The determination of the HOMO and LUMO energy levels and energy band gap of the modified particles are essential and this study presents the techniques used to obtain these values such as cyclic voltammetry and UV-VIS spectroscopy. This report focuses on the studies of particles containing clicked carbazole or oxadiazole moieties on their surface. It was found that PA particles with “clicked” oxadiazole moieties present a HOMO and LUMO energy levels of -5.55 eV

and -2.05 eV respectively, and the PA particles with “clicked” carbazole moieties present a HOMO energy level at -5.74 eV and a LUMO energy level at -2.44 eV.

REFERENCES

- (1) P. Rungta, Y. P. Bandera, V. Tsylkovsky, S. H. Foulger **2010**.
- (2) Burroughes, J. H.; Bradley, D. D. C.; Brown, A. R.; Marks, R. N.; Mackay, K.; Friend, R. H.; Burns, P. L.; Holmes, A. B. *Nature* **1990**, *347*, 539-541.
- (3) Evanoff, J., D. D; Carroll, J. B.; Roeder, R. D.; Hunt, Z. J.; Lawrence, J. R.; Foulger, S. H. *J. Polym. Sci. Pol. Chem.* **2008**, *46*, 7882-7897.
- (4) Evanoff, J., D. D; Lawrence, J. R.; Huebner, C. E.; Houchins, J. M.; Stevenson, B. J.; Foguth, A. L.; Carroll, J. B.; Foulger, S. H. *ACS Applied Materials & Interfaces* **2009**, *1*, 875-881.
- (5) Huebner, C. E.; Foulger, S. H. *Langmuir* **2009**, in press.
- (6) Huebner, C. F.; Carroll, J. B.; Evanoff, D.; Ying, Y.; Stevenson, B. J.; Lawrence, J. R.; Houchins, J. M.; Foguth, A. L.; Sperry, J.; Foulger, S. H. *J Mater Chem* **2008**, *18*, 4942-4948.
- (7) Evanoff, D. D.; Hayes, S. E.; Ying, Y.; Shim, G. H.; Lawrence, J. R.; Carroll, J. B.; Roeder, R. D.; Houchins, J. M.; Huebner, C. E.; Foulger, S. H. *Adv Mater* **2007**, *19*, 3507-3512.
- (8) Breed, D. R.; Thibault, R.; Xie, F.; Wang, Q.; Hawker, C. J.; Pine, D. J. *LANGMUIR* **2009**, *25*, 4370-4376.
- (9) Collman, J. P.; Devaraj, N. K.; Chidsey, C. E. D. *LANGMUIR* **2004**, *20*, 1051-1053.
- (10) Bock, V. D.; Hiemstra, H.; van Maarseveen, J. H. *European Journal of Organic Chemistry* **2006**, *1*, 51-68.

- (11) Lee, J. K.; Chi, Y. S.; Choi, I. S. *LANGMUIR* **2004**, *20*, 3844-3847.
- (12) Binder, W. H.; Sachsenhofer, R.; Straif, C. J.; Zirbs, R. *Journal of Materials Chemistry* **2007**, *17*, 2125-2132.
- (13) Binder, W. H.; Petraru, L.; Sachsenhofer, R.; Zirbs, R. *Monatshefte \protect{f}\u r} Chemie* **2006**, *137*, 835-841.
- (14) O. El-Gholabzouri, M. A. C.-V., R. Hidalgo-Alvarez **2006**, *291*, 30-37.
- (15) Xu, R. *Particuology* **2008**, *6* 112-115.
- (16) Micaroni, L.; Nart, F. C.; Hummelgen, I. A. *J. Solid State Electrochem.* **2002**, *7*, 55-59.
- (17) S. Schwarz, K. L., B. Keßler, U. Spiegler, E. Killmann, W. Jaeger *colloids and Surfaces A-Physicochemical and Engineering Aspects* **2000**, *163*, 17-27
- (18) Corporation, B. I. *zeta potential analyzer instruction manual*.
- (19) M.R. Gittings, D. A. S. *colloids and Surfaces a-Physicochemical and Engineering Aspects* **1998**, *141*, 111-117.
- (20) Lawrence, J. R.; Shim, G. H.; Jiang, P.; Han, M. G.; Ying, Y. R.; Foulger, S. H. *Adv Mater* **200**, *17*, 2344-+.
- (21) B. R. Midmore, R. J. H. *Journal of Colloid and Interface Science* **1988**, *122*.
- (22) G. Tuin, J. H. J. E. Sender., H. N. Stein *Journal of Colloid and Interface Science* **1996**, *179*, 522-531.
- (23) Franks, G. V. *Journal of Colloid and Interface Science* **2002**, *249*.

- (24) P.S. Bolt, J. W. G., R.H. Ottewill *langmuir* **2005**, 21, 9911-9916.
- (25) Vanderhoff, J. W. *Pure and Applied Chemistry* **1980**, 22, 1263-1273.
- (26) M. E. Labib, A. Robetson. *Journal of Colloid and Interface Science* **1979**, 77, 151-161.
- (27) Vanderhoff, J. W. *Science and technology of polymer colloids, Preparation and reaction engineering* **1983**, 1.
- (28) J. Syne-Masui, A. Watillon . *journal of Colloid and Interface Science* **1975**, 75,n°3, 479-502.
- (29) A. A. Kamel, M. S. El.-Aasser., J. W. Vanderhoff *Journal of Colloid and Interface Science* **1982**, 87, n°2, 537-542.
- (30) H. G. Van Den Hul, J. W. Vanderhoff. *Journal of Colloid and Interface Science* **1968**, 28, n°2, 336-337.
- (31) A. J. Bard, L. R. Faulkner. *Wiley* **1980**, 634.
- (32) Trasatti, S. J. *Electroanalysis chemistry* **1983**, 150:1.
- (33) B. Jo'm, K. Sum. *plenum press* **1983**, 78.
- (34) Meng, H. *Synth Met* **1999**.
- (35) Yingliang Liu, S. X., Jianghui Li, Yuanrong Xin, Guoxin Zhao, Baoxian Ye2 and Shaokui Cao *POLYMERS FOR ADVANCED TECHNOLOGIES* **2008**, 19, 793-800.
- (36) Macit, H. *Journal of Applied Polymer Science* **2005**, , Vol. 96, 894-898 (2005).
- (37) Oral *synth Met* **2009**.

- (38) Yeh, K. M.; Lee, C. C.; Chen, Y. J. *Polym. Sci. Pol. Chem.* **2008**, *46*, 5180-5193.
- (39) Cacialli, F.; Li, X. C.; Friend, R. H.; Moratti, S. C.; Holmes, A. B. *Synth Met* **1995**, *75*, 161-168.
- (40) J. H. Kim, H. L. *Synthetic Metals* **2004**, *143*, 13-19.
- (41) Lee, H.-s. *THIN SOLID FILMS* **2000**.
- (42) Peng, Z. H.; Bao, Z. N.; Galvin, M. E. *Adv Mater* **1998**, *10*, 680-684.
- (43) R. Cervini, X.-C. Li., G.W.C. Spencer, A. B. Holmes, C. Moratti and R. H. Friend *synth Met* **1997**, 359-360.
- (44) P. WANG, H. J., Q. YANG, W. LIU, Z. SHEN, X. CHEN, X. FAN, D. ZOU, Q. ZHOU *journal of Polymer Science Part \protect{A}-I-Polymer Chemistry* **2009**, *47*, 4555–4565
- (45) B. Xu, Y. P., J. Zhang, Z. Peng *Synth Met* **2000**, 337–345.